CrystEngComm

Accepted Manuscript

ROYAL SOCIETY OF CHEMISTRY

www.rsc.org/crystengcomm

Engineering of crystal surfaces and subsurfaces by framework biomineralization protein phases.†

Eric P. Chang,[a] Jennie A. Russ,[b] Andreas Verch,[c] Roland Kröger,[c] Lara A. Estroff,[b] and John Spencer Evans[a]*

Received (in XXX, XXX) Xth XXXXXXXXX 200X, Accepted Xth XXXXXXXXX 200X
First published on the web Xth XXXXXXXXX 200X
DOI: 10.1039/b00000000x

We report an interesting phenomenon whereby a framework mollusk shell nacre protein, n16.3, facilitates a two-stage crystal growth process. This protein forms phases that permit initial calcite growth, then via direct contact introduce textured mineral overgrowth to these core crystals in a directional fashion, and, create subsurface nanoporosities within these crystals. This phenomenon is an example of crystal modification and assembly directed by a biomineralization protein phase and we believe this framework protein-driven process is important for the assembly of the nacre shell layer. Similar phase-based approaches could be used to engineer a variety of inorganic crystals for technological applications.

Nature uses proteins to create three-dimensional mineralized structures that offer several important functions for biosurvival.[1-18] However, there is uncertainty with regard to the role(s) that proteins play within different biomineral formation processes. For example, the nacre framework proteome[7,10-15] are a collection of proteins affiliated with the beta-chitin polysaccharide – silk-like fibroin gel matrix that coats the exterior of aragonite tablets in the nacre layer of some mollusk shells.[16] It is known that this macromolecular gel-like coating is an important medium for controlling calcium carbonate nucleation.[16,17] Hence, the framework proteome may play a role in nacre mineralization events directed by this gel matrix phase. Unfortunately, there is very little information available regarding the framework proteome and its participation in the nacre layer formation process. As a result, our present understanding of mollusk shell biomineralization is limited, and this in turn prevents us from developing promising materials science applications based upon the shell engineering process.

Recent studies reveal that the certain members of the nacre framework proteome, such as n16.3 (108 AA, MW = 12.9 kDa, pI = 4.84, *Pinctada fucata*, Electronic Supplementary Information, Fig S1),[10,12,15] feature cationic and anionic amino acids, intrinsic disorder (i.e., lack of internal protein folding) and short cross-beta strand regions (Electronic Supporting Information, Figs S1, S2) which promote protein aggregation into gel phases.[18] The protein gel phase can nucleate very limited quantities of single crystal aragonite,[15] and in the early stages of mineralization these phases capture and organize mineral nanoparticles in solution and modulate the post-nucleation solubilities of these organized deposits.[18] However, it is not known if these same protein phases can control the growth of existing crystals. Establishing the performance of protein gel phases at different stages of the mineralization process is an important step for developing materials based upon the mollusk shell model.

In this Communication, we report on the capability of n16.3 gel-like protein phases to direct a two-stage crystal growth process. First, the protein phases allow typical rhombohedral calcite crystals form. Subsequently, the protein phases deposit onto the crystals and promote textured overgrowth on these core crystals along the [104] direction (Fig 1). During this two-stage process the protein phases introduce subsurface nanoporosities to the overgrowth regions of these same growing crystals (Fig 2). Thus, nacre framework protein gel phases can direct mineral assembly in solution[18] *and* on crystal surfaces. We note that crystal growth modifications have also been observed in other gel-based mineralization systems.[19-22]

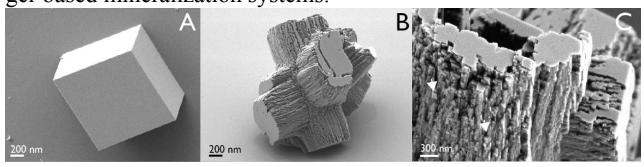

Fig 1. A) Representative calcite crystals obtained from protein-deficient controls. B) Representative mineral deposits generated by r-n16.3 in 1 hr, revealing symmetric mineral projections and textured single crystal overgrowth (C, examples denoted by arrows).

For the purposes of this study we utilized sealed carbonate/bicarbonate mineralization assays (Electronic Supplementary Information)[8,18] that reproducibly generate calcite with well-defined {104} surfaces for EM examination and thus avoid imaging complications arising from vaterite and aragonite. In the presence of recombinant n16.3 (r-n16.3), whose sequence represents the mature, processed form of n16.3,[15,18] we observe the formation of unique three-dimensional symmetric mineralized structures (Fig 1B.) Physical characterization methods revealed that the mineralized structures are calcite (Electronic Supplementary Information, Fig S3-S6, Table S1). These symmetric mineralized structures represent > 80% of the total crystals produced by r-n16.3 under these assay conditions and thus these symmetric structures arise from a protein-driven process.

A closer examination of these r-n16.3 – generated mineral structures revealed some interesting features. First, we observe that each mineral extension consists of irregular overgrowth regions (Fig 1C). These regions possess gaps or spaces and using electron diffraction we determined that the mineral phase in these regions is single crystal calcite (Electronic Supplementary Information, Fig S4). Second, focused-ion beam (FIB) milling of the mineral extensions (Fig 2; Electronic Supplementary Information, Fig S7) reveal a greater number of subsurface

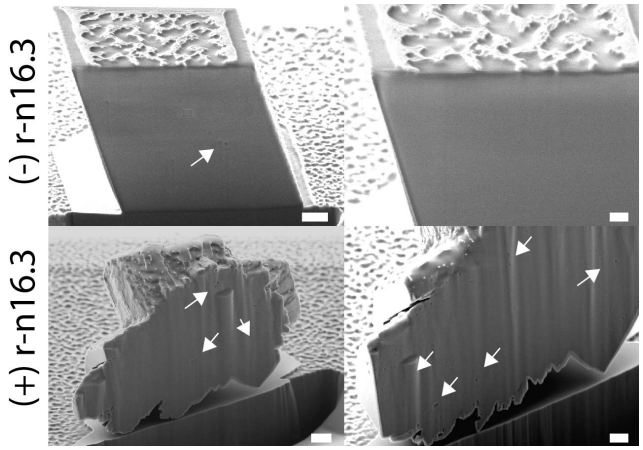

Fig 2. Representative SEM images of FIB sectioned Ir-coated crystals obtained from protein – deficient and r-n16.3-containing assays. White arrows denote locations of subsurface voids (enlargement of these regions can be found in Electronic Supplementary Information, Fig S7). Note the larger number of subsurface porosities in the r-n16.3 crystal compared to controls. Scalebars = 200 nm.

nanoporosities, particularly in peripheral regions, compared to calcite crystals obtained from protein-deficient assays. We believe that these nanoporosities represent the surface gaps or spaces (Fig 1C) that subsequently became incorporated into the bulk crystal during subsequent stages of mineral overgrowth that occurred in the presence of r-n16.3.

In r-n16.3-containing assays we also observed phases that deposit onto Si wafer supports (Fig 3A) and are associated with the mineralized structures themselves (Fig 3B). These phases feature the typical spheroidal-fibrillar subunit morphologies associated with r-n16.3 phases (Fig 3A).[15] Using X-ray microanalysis, we detected elemental protein-associated C, O, and N signals associated with these phases (Electronic Supplementary Information, Fig S3). Together, these data confirm that these captured phases are r-n16.3 assemblies.[15,18]

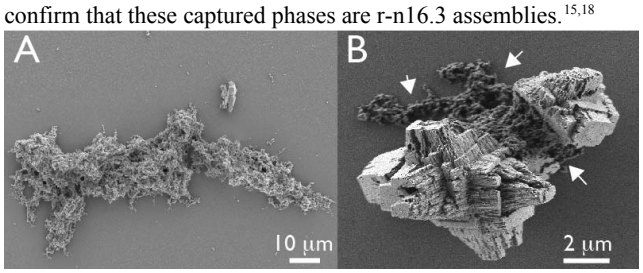

Fig 3. A) Representative r-n16.3 gel phases captured on Si wafers during 1 hr mineralization assay. B) r-n16.3 gel phase (white arrow) associated with nucleating pseudo-symmetric mineral structures. Note that SEM sample preparation induces dehydration and thus significantly alters the appearance and dimensions of the protein phases.[18]

From the foregoing we suspected that mineralized structures (Fig 1B, 3B) were formed via r-n16.3 protein phase interactions with growing calcite crystals. To confirm this, we performed time-resolved assays (1, 5, and 15 min duration) and monitored the formation of mineral and r-n16.3 protein phases (Fig 4). Typical rhombohedral polycrystalline calcite crystals are observed at the end of 1 minute, and many of these crystals feature {104} surface-adsorbed r-n16.3 protein gel-like phases. Due to SEM sample dehydration, these gel phases appear collapsed. Interestingly, some of the protein phases collect near the intersections of the {104} surfaces (Fig 3). At 5 min we observe continued protein deposition and crystal growth along the [104] direction. This growth behavior is also similar to that reported for the n16.3 – derived n16N polypeptide which induces crystal growth in new directions compared to controls.[23] By 15 minutes the crystal structures start to resemble those obtained at 1 hr (Fig 1) and now exhibit the familiar overgrowth regions. Most importantly, we observe that the r-n16.3 phases are in contact with the {104} surfaces and overgrowth regions. Thus, we affirm that the mineralized structures (Fig 1) are created by the repetitive deposition of r-n16.3 gel-like phases onto calcite crystals (Fig 4).

In conclusion, we establish that a mollusk shell nacre framework protein phase not only organizes mineral nanoparticles in solution[15,18] but also allows "core" calcite crystals to form and then modifies their growth direction, creates surface texture, and introduces subsurface nanoporosities (Fig 1, 2, 4). These features result from repetitive protein gel-phase deposition on the surfaces of the calcite crystals (Fig 4). Given that n16.3 possesses both anionic and cationic amino acids (Electronic Supplementary Information, Figs S1, S2),[15,18] the protein gel phase would be quite capable of promoting calcium and bicarbonate/carbonate ion sequestration at crystal surfaces, which in turn would direct nucleation and mineral overgrowth in the vicinity of the protein gel phase. We believe that the formation of single crystal calcite in the overgrowth regions (Fig 1; Electronic Supplementary Information, Fig S4) are guided by the underlying calcite foundation (Fig 4). In other words, the underlying calcite crystal orients the mineral nanoparticles that nucleate within the r-n16.3 gel phase.[18] In conclusion, the n16 protein family[10,12,15,18] is an example of a gel-like macromolecular system[19-22] that manipulates the early and later stages of the nucleation and crystal growth processes. It is likely that protein[8,15,18] or polymeric[2,19,20] phase technologies will offer an interesting route for introducing new dimensional, directional, and physical properties to nucleating crystals.

The introduction of subsurface nanoporosities by r-n16.3 during crystal nucleation is an intriguing feature (Fig 2; Electronic Supplementary Information, Fig S7). We note that similar nanoporosities have been observed within prismatic calcite in certain mollusks.[24] Based upon the surface (Figs 1,4) and cross-sectional profiles (Fig 2) we propose that the nanoporosities originated from the intercrystalline gaps or spaces that formed during the early stages of r-n16.3-induced overgrowth. As mineralization proceeds, the majority of these gap or spaces become filled in with mineral overgrowth over time. However, given that the r-n16.3 protein phases are found in direct contact with the overgrowth surfaces and intercrystalline spaces (Fig 3B, Fig 4), it is plausible that the protein phase became entrapped within some of these gaps or spaces and could not be expelled during subsequent mineral phase overgrowth. If true, then the nanoporosities in calcite (Fig 2) represent persistent enclaves containing r-n16.3 protein phases (i.e., intracrystalline inclusions).[24] We intend to verify this possibility in subsequent studies.

Notes and references

[a]*Laboratory for Chemical Physics, Center for Skeletal Sciences, New York University New York, NY (USA). Fax: 01 995 4087; Tel: 01 347 753 1955; E-mail: jse1@nyu.edu*
[b]*Department of Materials Science and Engineering, Cornell University Ithaca, NY (USA) Tel: 01 607 254 5256; E-mail: lae37@cornell.edu*

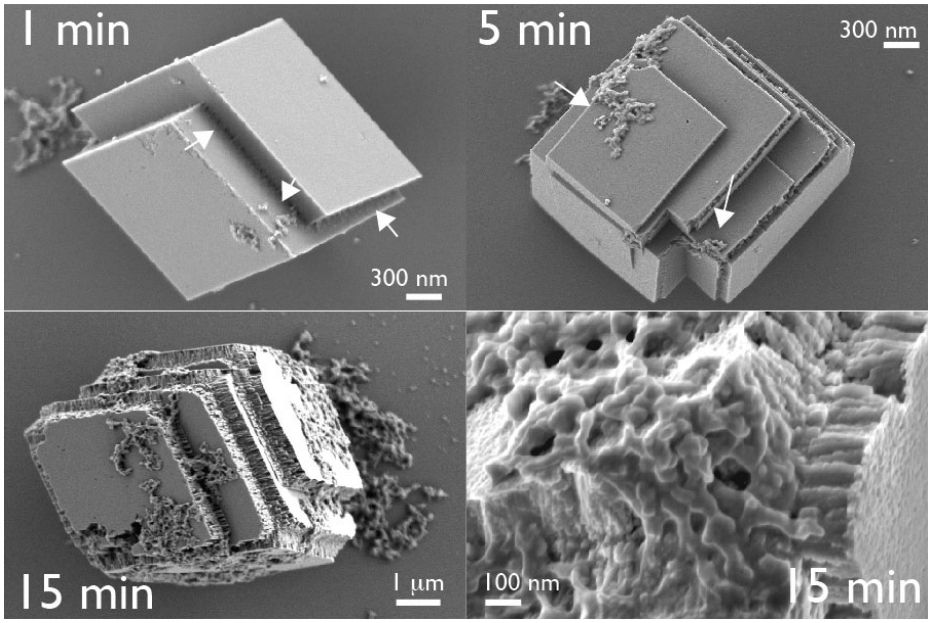

Fig 4. SEM images of mineral deposits and protein phases forming in time-resolved mineralization assays. Supernatant sampling was performed at 1, 5, and 15 min intervals after initial mixing of ionic and protein solutions. Note the presence of protein phases on Si wafer backgrounds. White arrows denote location of protein phases captured on crystal surfaces. Close-up image shows r-n16.3 phase coating in regions where single crystal calcite is forming.

[c]*Department of Physics, University of York, York (UK). Tel: 44 1904 324622; E-mail: roland.kroger@york.ac.uk.*

Portions of this research (mineral assays, SEM, TEM, FIB) were supported by the U.S. Department of Energy, Office of Basic Energy Sciences, Division of Materials Sciences and Engineering under award DE-FG02-03ER46099 to JSE. LAE acknowledges support from NIH/NCI Grant RO1 CA173083. The microRaman studies made use of the Cornell Center for Materials Research Shared Facilities (NSF MRSEC DMR-1120296). This paper represents contribution number 75 from the Laboratory for Chemical Physics.

†Electronic Supplementary Information (ESI) available: Experimental section detailing characterization methods, protein preparation, and mineralization assay conditions. Supporting Figures S1-S7, Table S1. See DOI: 10.1039/b000000x/

1 H.A. Lowenstam, S.Weiner, in *On Biomineralization*, Oxford University Press, Oxford, U.K., 1989.
2 L.B. Gower, *Chem. Rev*. 2008, **108**, 4551; S.E. Wolf, J. Leiterer, R. Pipich, F. Barrea, F. Emmerling, W.J. Tremel, *J. Am. Chem. Soc*. 2011, **133**, 12642.
3 E.M. Pouget, P.H.H. Bomans, J.A.C.M. Goos, P.M. Frederick, G. de With, N.A.J.M. Sommerdijk, *Science* 2009, **323**, 1455.
4 D. Gebauer, A. Volkel, H. Cölfen, *Science* 2008, **322**, 1819.
5 A.F. Wallace, L.O. Hedges, A. Fernandez-Martinez, P. Raiteri, J.D. Gale, G.A. Waychunas, S. Whitelam, J.F. Banfield, J.J. De Yoreo, *Science* 2013, **341**, 885.
6 M.M. Murr, D.E. Morse, Proc. Natl. Acad. Sci. USA 2005, 102, 11657; A. Scheffel, N. Poulsen, N., S. Shian, N. Kröger, *Proc. Natl. Acad. Sci. USA* 2011, **108**, 3175.
7 J.S. Evans, *Cryst. Eng Comm*. 2013, **15**, 8388; J.S. Evans, *Chem. Rev.* 2008, **108**, 4455.
8 C.J. Stephens, Y.Y. Kim, S.D. Evans, F.C. Meldrum, H.K. Christenson, *J. Am. Chem. Soc.* 2011, **133**, 5210; C.J. Stephens, S.F. Ladden, F.C. Meldrum, H.K. Christenson, *Adv. Mater.* 2010, **20**, 2108.
9 F. Nudelman, K. Pieterse, A. George, P.H.H. Bomans, H. Friedrich, L.J. Brylka, P.A.J. Hilbers, G. DeWith, N. A. J. M. Sommerdijk, *Nature Materials* 2010, **9**, 1004.
10 S. Kinoshita, N. Wang, H. Inoue, K. Maeyama, K. Okamoto, K. Nagai, H. Kondo, I. Hirono, S. Asakawa, S. Watabe, *PLOS One* 2011, **6**, 1.
11 B. Marie, C. Joubert, A. Tayale, I. Zanella-Cleon, C. Belliard, D. Piquemal, N. Cochennec-Laureau, F. Marin, Y. Gueguen, C. Montagnani, *Proc. Natl. Acad. Sci USA* 2012, **109**, 20986; C. Montagnani, C., B. Marie, F. Marin, C. Belliard, F. Riquet, A. Tayale, I. Zanella-Cleon, E. Fleury, Y. Geuguen, D. Piquemal, N. Cochennec-Laureau, *ChemBioChem* 2011, **12**, 2033.
12 C. Nogawa, H. Baba, T. Masaoka, H. Aoki, T. Samata, Gene 2012, 504, 84; L.D. Gardner, D. Mills, A. Wiegand, D. Leavesley, A. Elizur, *BMC Genomics* 2012, **12**, 455; D. Fang, G. Xu, Y. Hu, C. Pan, L. Xie, R. Zhang, *PLOS One* 2011, **6**, 1; M. Suzuki, K. Saruwatari, T. Kogure, Y. Yamamoto, T. Nishimura, T. Kato, H. Nagasawa, *Science* 2010, **325**, 1388; T. Samata, N. Hayashi, M. Kono, K. Hasegawa, C. Horita, S. Akera, *FEBS Letters* 1999, **462**, 225; S. Berland, A. Marie, D. Duplat, C. Milet, J.Y. Sire, L. Bedouet, *ChemBioChem*. 2011, **12**, 950.
13 G. Zhang et al., *Nature* 2012, **490**, 49.
14 J.S. Evans, *Bioinformatics* 2012, **28**, 3182.
15 C.B. Ponce, J.S. Evans, *Crystal Growth and Design* 2011, **11**, 4690.
16 E.C. Keene, J.S. Evans, L.A. Estroff, *Crystal Growth and Design* 2010, **10**, 5169.
17 Y. Levi-Kalisman, G. Falini, L. Addadi, S. Weiner *J. Struct. Biol.* 2001, **135**, 8; F. Nudelman, E. Shimoni, E. Klein, M. Rousseau, X. Bourrat, E. Lopez, L. Addadi, S. Weiner, *J. Struct. Biol*. 2008, **162**, 290.
18 I. Perovic, E.P. Chang, M. Lui, A. Rao, H. Cölfen, J.S. Evans, *Biochemistry* 2014, **53**, 2739.
19 I. Sethmann, A. Putnis, O. Grassmann, P. Loebmann, *Am. Miner.* 2005, **20**, 1213.
20 F.F. Amos, D.M. Sharbaugh, D.R. Talham, L.B. Gower, M. Fricke, D. Volkmer, *Langmuir* 2007, **23**, 1988; M. Bewernitz, D. Gebauer, J. Long, H. Cölfen, L.B. Gower, *Faraday Discuss.* 2012, **159**, 291.
21 L. Addadi, D. Joester, F. Nudelman, S. Weiner, *Chem. Eur J*. 2006, **12**, 980.
22 A. Gal, W. Habraken, D. Gur, P. Fratzl, S. Weiner, L. Addadi, *Angew. Chem. Int. Ed*. 2013, **52**, 4867.
23 I.W. Kim, M.R. Darragh, C. Orme, J.S. Evans, *Crystal Growth and Design* 2006, **5**, 5.
24 H. Li, H.L. Xin, D.A. Muller, L.A Estroff, *Science* 2009, **326**, 1244.